JAERI-Research
2004-005

ANALYSIS OF IMPURITIES IN BERYLLIUM, AFFECTING EVALUATION OF THE TRITIUM BREEDING RATIO

March 2004

Yury M.VERZILOV, Kentaro OCHIAI, Satoshi SATO
Masayuki WADA*, Michinori YAMAUCHI
and Takeo NISHITANI

日本原子力研究所
Japan Atomic Energy Research Institute

本レポートは，日本原子力研究所が不定期に公刊している研究報告書です。
入手の問合わせは，日本原子力研究所研究情報部研究情報課（〒319-1195　茨城県那珂郡東海村）あて，お申し越しください。なお，このほかに財団法人原子力弘済会資料センター（〒319-1195　茨城県那珂郡東海村日本原子力研究所内）で複写による実費頒布をおこなっております。

This report is issued irregularly.
Inquiries about availability of the reports should be addressed to Research Information Division, Department of Intellectual Resources, Japan Atomic Energy Research Institute, Tokai-mura, Naka-gun, Ibaraki-ken, 319-1195, Japan.

編集兼発行　　日本原子力研究所

JAERI-Research 2004-005

Analysis of Impurities in Beryllium, Affecting Evaluation of the Tritium Breeding Ratio

Yury M.VERZILOV※, Kentaro OCHIAI, Satoshi SATO, Masayuki WADA*
Michinori YAMAUCHI and Takeo NISHITANI

Department of Fusion Engineering Research
(Tokai Site)
Naka Fusion Research Establishment
Japan Atomic Energy Research Institute
Tokai-mura, Naka-gun, Ibaraki-ken

(Received January 30, 2004)

In most conceptual fusion power reactor designs, it is proposed to use beryllium as a neutron multiplier in the blanket. Detailed chemical composition of beryllium is necessary for evaluation of the tritium breeding ratio, and estimating the activation and transmutation of beryllium in the fusion reactor. In the present report, special attention was paid to a detailed analysis of impurities in beryllium, relevant to the tritium breeding ratio evaluation. Two different methods were used for the study of impurities: an analysis of the local sample by the ICP-MS method, and an integral analysis of the beryllium assembly, using the pulsed neutron method. The latter method was proposed as the most effective way of analyzing the integral effect of impurities in beryllium on production of the tritium on the lithium-6. The evaluation of the integral effect was based on time behaviour observations of the thermal neutron flux, following the injection of a burst of D-T neutrons into the beryllium assembly. Structural beryllium grade (S-200-F, Brush Wellman Inc.) was used in the study. The influence of the impurities has resulted in a smaller experimental reaction rate for production of the tritium on lithium-6, due to an increase in the parasitic neutron absorption. Experimental data was compared with the reference data and the MCNP Monte Carlo calculations using the JENDL-3.2 data set. Results indicate, that the measured absorption cross section of thermal neutrons in beryllium blocks is approximately 30% larger than the calculated value, based on the data, specified by the manufacturing company. ICP-MS analysis indicated that the impurities include elements such as Li, B, Cd and others. These elements affect the absorption cross section even if the content of impurities is less than 10 ppm.

Keywords: D-T Neutrons, Fusion Reactor, Blanket, Beryllium, Impurities, Tritium Breeding Ratio, Pulsed Neutron Technique, FNS

※ JAERI Research Fellow
* Startcom Co., Ltd.

トリチウム増殖比に影響するベリリウム中の不純物分析

日本原子力研究所那珂研究所核融合工学部
Yury M.VERZILOV※・落合　謙太郎・佐藤　聡・和田　正行*・山内　通則・西谷　健夫

(2004年1月 30 日受理)

ほとんどの核融合炉の概念設計において、ブランケットにおける中性子増倍材としてベリリウムの利用が提案されている。その核融合炉のトリチウム増殖比やベリリウムの放射化と核変換の評価においてはベリリウムの詳細な化学組成が必要である。本報告ではトリチウム増殖比の評価に関連する詳細な不純物分析に特に注目した。ここでは2つの異なった方法で不純物を調べた。1つはICP質量分析法による一部の試料の分析であり、もう1つはパルス化中性子を用いたベリリウム体系の積分的分析である。特に後者は ^{6}Liによるトリチウム生成に対するベリリウム中の不純物の積分的効果の最も有効な分析法として提案した。D-T中性子のパルスをベリリウム体系に入射し、その後の熱中性子密度の時間変化を観測することにより積分的効果を評価した。本研究では構造材級ベリリウム（ブラッシュウェルマン社S-200-F）を使用した。この不純物の影響は寄生的な中性子の吸収により実験で得られた ^{6}Liによるトリチウム生成の反応率を減少させる。核データセットJENDL-3.2を用いたMCNPモンテカルロ計算と実験値を比較した結果、測定された吸収断面積は製作会社の特性値から評価した値より約30%大きくなった。ベリリウム中のLi, B, Cd等の不純物はたとえ10ppm以下でも吸収断面積に影響する。

那珂研究所（東海駐在）：〒319-1195 茨城県那珂郡東海村白方白根2-4
※　原研リサーチフェロー
*　スタートコム（株）

Contents

目　次

1. Introduction

Beryllium is a high priority material utilized in the field of fusion technologies. In most conceptual fusion power reactor designs, it is proposed to use beryllium as a neutron multiplier in the blanket [1]. Neutron multipliers are required in order to compensate for parasitic neutron losses, and therefore to enable net tritium production. In addition, beryllium is an excellent neutron moderator with an extremely low absorption cross section for thermal neutrons. In such conditions, tritium production mostly occurs through absorption of thermal neutrons by lithium-6, according to the reaction $^{6}Li(n,\alpha)^{3}H$. However, thermal neutrons can be easily absorbed by other elements as well, if they are presented in beryllium as impurities that increase the absorption cross section. At a maximum, the impurities in beryllium can increase the absorption cross section by up to 30 times [2]. This impurity effect decreases the number of thermal neutrons, and as a result, the tritium production is decreased. Considering that such impurities can exist in structural beryllium grades, beryllium blocks (S-200F, Brush Wellman Inc.) used for the blanket benchmark experiments were studied with the purpose of qualification and validation. Generally, the inductively coupled plasma mass spectrometry method is suitable for the study, however, due to the wide spectrum and range of expected impurities, and their non-uniform distributions in beryllium, the study will be quite a lengthy and laborious procedure. In such circumstances, it is useful to use a method which is able to quickly, easily and precisely evaluate the integral effect of impurities affecting evaluation of the tritium breeding ratio.

2. Chemical Composition of Structural Beryllium Grades and the Impurity Effect on Tritium Production

Structural grades S-65C, S-200F and S-200E (Brush Wellman Inc.) are being considered for use in ITER [3]. Manufacturer information concerning the composition of these grades, is shown in Table 1. In typical specifications, the main impurity elements are characterized by a high concentration, about 1000 ppm. Minor impurities

are commonly not specified in detail. Instead, the total impurity level, of about 400 ppm, is shown in the last row of Table 1.

Table 1

Specification of chemical compositions for structural beryllium grades

Chemical composition	S-65B/S-65C	S-200F	S-200E
Be, min %	99.0	98.5	98.0
BeO, max %	1.0	1.5	2.0
Al, max ppm	600	1000	1600
C, max ppm	1000	1500	1500
Fe, max ppm	800	1300	1800
Mg, max ppm	600	800	800
Si, max ppm	600	600	800
Other max ppm	400	400	400

This level isn't dependent on the beryllium grade. Very limited information concerning the content of minor impurities is available. Various studies [4-7] have shown that impurities can include elements such as Li, B, Cl, Cr, Mn, Co, Cd, Dy, Th, U and others. Data were gained from a variety of studies, mainly concerning purification procedures of the high quality beryllium, as shown in Table 2. Impurity levels represent only the lower limit of potential impurities in structural beryllium. Most probably, the actual impurity content in commercially available beryllium grades is significantly higher.

Table 2.

The chemical composition of commercial, vacuum melted and distilled high purity beryllium

Chemical composition	Purification procedure			PF-60**
	Vacuum melted [5]	Vacuum melted plus refined [6]	Vacuum distilled [5]	
Be, %	99.5	99.7	99.9	99.0
BeO, ppm				8000
Fe, ppm	1100	250	110	700
Al, ppm	600	200	20	500
Mg, ppm	500		8	500
Si, ppm		100	20	400
C, ppm	400	150		700
Cr	90	20	50	100
Co	2			10
Cu		10	50	100
Pb				20
Mn	70	20	35	120
Mo				20
Ni	130	125	70	200
Ca		< 200	30	100
Cl		< 50	50	
Ag	5			10
N			10	
B	1.2			3
Cd	0.5			2
Li	1			3
U				25-140
Th				< 2

* Empty space in the column shows absence of data.

** Data is specified for PF-60 (Brush Wellman Inc.)

An additional study, with the use of neutron activation and gamma spectrometry [4], was done to determine amount of uranium in beryllium. Results show that even in relatively pure beryllium, a uranium concentration of about 20 ppm was found. Some of the elements listed in Table 2 tend to have a significant effect on the absorption cross section of thermal neutrons, in spite of the low impurity level, caused by a high value of the absorption cross sections of the elements. It is possible to estimate the significance of the effect, using the impure beryllium to pure beryllium ratio of the total macroscopic absorption cross sections, R. Results of calculations of R for impurities, which are characterized by a high absorption cross section, are presented in Table 3.

Table 3.

The effect of minor impurities on the ratio of macroscopic absorption cross section of impure to pure beryllium, R.

Composition			R
Be, %	Impurity		
	Element	Level, ppm	
100	---	0	1.00
99.99	B	5	1.43
99.99	Gd	5	2.78
99.99	Cd	5	1.15
99.99	Li	5	1.06
99.99	Cl	100	1.11
99.99	Co	100	1.08
99.99	Mn	100	1.03
99.99	All the above	320	3.63

As indicated in this table, even a small amount of impurities, less than 10 ppm, can significantly increase the total absorption cross section in beryllium.

As an example of the influence of the parasitic absorption in the beryllium moderator on the tritium production, an estimation of the tritium production rate on lithium-6, TPR-6, was performed for the pure beryllium assembly, irradiated by D-T neutrons. The parasitic absorption was simulated by boron at a level of 5 ppm, a

concentration corresponding to a 40% increase of the absorption cross section. The ratio of TPR-6 in the impure beryllium to pure beryllium is presented in Fig.1. The parasitic absorption decreases the TPR-6 by about 5% on the surface of assembly (Fig. 1). This effect has a tendency to decrease the TPR-6 to a deeper location, due to moderation and thermalization of neutrons, as a result of the increasing absorption cross section, which follows the 1/v-law. Nevertheless, the impurity effect depends on the blanket design, volumetric ratio of lithium and beryllium, and enrichment of lithium.

3. Physical Specification of Beryllium Blocks

For integral benchmark experiments, that were performed in the FNS facility, standard grade beryllium blocks (S-200-F, Brush Wellman Inc.) were used. The standard grade is to be produced through consolidation of beryllium powder by vacuum hot pressing. The blocks are machined from the vacuum hot pressed material. In total, there are nine types of blocks with different dimensions, listed in Table. 4.

Table 4.

The beryllium blocks which were used for integral benchmark experiments

Type	Overall volume, cm^3	Dimension, cm			Average density, g/cm^3
		a	b	c	
Monolithic blocks					
I	$9.52 \cdot 10^4$	5.08	5.08	5.08	1.833
II		5.08	5.08	10.16	1.845
III		5.08	5.08	2.54	
IV	$9.18 \cdot 10^3$	10.16	10.16	1.27	1.848
V		10.16	10.16	5.08	
VI	$1.44 \cdot 10^4$	2.566	7.655	305	1.837
Glued blocks					
VII	$3.62 \cdot 10^4$	2.57	7.62	15.26	1.829
VIII	$5.21 \cdot 10^4$	15.25	15.25	5.14	1.822
IX		15.23	7.62	5.11	1.832

4. Sample Analysis

4.1. Specification Data Provided by the Manufacturing Company

The beryllium material was manufactured in the late 50`s by Brush Wellman Inc. Specifications obtained from the manufacturing company are shown in Table 5. The presented beryllium sample was analyzed on January 17th, 1984.

Table 5.

Chemical composition of the beryllium sample

Chemical composition	Content
Be, %	98.82
BeO, %	1.13
C, ppm	840
Fe, ppm	1250
Al, ppm	710

4.2. ICP-MS Measurements

In order to expand knowledge, concerning minor impurities in beryllium, the inductively coupled plasma mass spectrometry (ICP-MS) method was used for analysis of the sample. The study was completed by the Analytical Chemistry Laboratory (Department of Material Science) in JAERI [7]. Results of the analysis are presented in Table 6. Some of the elements were detected, though their quantities were not measured absolutely (indicated by symbol "S").

Table 6.

Chemical composition of the S-200-F standard grade beryllium measured with the ICP-MS method

Element	Content	Element	Content
Be, %	97.9±0.8	Ni, ppm	250±30
Li, ppm	< 1	Zr	S
B, ppm	< 3	Nb	S
Mg, ppm	110±5	Mo	S
Al, ppm	570±50	Cd, ppm	< 1
Sc	S	Dy	S
Ti	S	Ta	S
V	S	W	S
Cr	S	Hg	S
Mn, ppm	96±5	Pb	S
Fe, ppm	1300±70	Th, ppm	1.5±0.1
Co	S	U, ppm	82±3

Results obtained from the spectroscopic study, can introduce some uncertainties to calculations of the tritium production rate, due to the sensitivity level of the technique, therefore not being able to meet the benchmark requirements for the integral experiment. Besides, additional uncertainties can exist as well, due to the non-uniform impurity distribution, since only one sample of the beryllium material was analyzed. In such circumstances, for qualification and validation purposes, measurements of the integral effect seem very useful.

5. Integral Non-Destructive Method for Impurity Analysis

The non-destructive, pulsed neutron method was chosen with the following constrains in mind. First, it is useful to estimate the total effect of impurities, which increase the macroscopic absorption cross section of thermal neutrons, since the effect

directly affects the tritium breeding ratio on lithium-6. Secondly, it is reasonable to measure the integral effect of impurities, in order to avoid a future problem concerning uniformity of impurity distributions. The effectiveness of this method is based on the following facts:

- ✓ all beryllium blocks, used for the benchmark experiments are suitable for estimation of the integral impurity effect;
- ✓ the total macroscopic absorption cross section for thermal neutrons can be measured;
- ✓ high accuracy of experimental results;
- ✓ fast and simple experimental procedures.

Originally, the pulsed neutron method was developed for precise determination of the neutron diffusion parameters in the moderator media [8]. Since then, it was used successfully in a variety of applications, including thermal absorption cross section measurements.

5.1. Basic Principles of the Method

The principle of the neutron pulsed method is described in detail in Ref. [8]. In essence, the method consists of time behavior observations of the neutron flux, following the injection of a burst of neutrons into the moderator. Fast neutrons inside the assembly rapidly slow down to thermal velocities (the slowing-down time in beryllium ~ 100 μsec). When the neutrons approach thermal equilibrium with the moderator, they continue to leak slowly out of the assembly or can be absorbed. The thermal neutrons decay according to the law:

$$\Phi(t) \approx e^{-\alpha t}. \tag{1}$$

The constant $1/\alpha$ is the effective thermal neutron lifetime. If the geometrical dimensions of the moderator are characterized by its buckling parameter B^2, the experimentally observed decay constant can be presented the following way:

$$\alpha = \alpha_0 + \left(D - CB^2\right) \cdot B^2, \tag{2}$$

(3)

$$\alpha_0 = v_0 \cdot \Sigma_a^{total}(v_0), \text{ for } 1/v \text{ - absorption}$$

where:

α_0 – is the decay constant which would be observed in an infinite medium and is entirely dependent on absorption entirely dependent on absorption ($\Sigma_a^{total}(v) = \sigma_a^{Be}(v) \cdot n^{Be} + \sum_{Impurities} \sigma_a^i(v) \cdot n^i$, σ_a^i - cross section, and n^i - number of nuclei per unit volume);

D – diffusion coefficient;

v_0 – neutron velocity (2200 m/sec);

The term –"CB^2" is a small correction to the diffusion coefficient, which describes the diffusion cooling. In a finite moderator, the neutron equilibrium temperature lies below the moderator temperature, due to the fact, that the leakage rate increases with velocity. Geometrical buckling for the parallelepipedal assembly can be estimated with the following formula:

(4)

$$B^2 = \pi^2 \cdot \left(\frac{1}{\tilde{a}^2} + \frac{1}{\tilde{b}^2} + \frac{1}{\tilde{c}^2} \right)$$

where:

$\tilde{a}, \tilde{b}, \tilde{c}$ – "effective dimensions", $\tilde{a} = a + 1.42\lambda_{tr}$;

a, b, c – actual dimensions;

λ_{tr} – transport mean free path.

Hence, measurement of the decay constant α of the thermal neutron flux for the fixed size of the moderating assembly and known diffusion parameters for beryllium, will permit determination of the absorption cross section. As an example of influence of the parasitic absorption in the beryllium moderator on the decay constant, an estimation of the time distribution of the thermal neutrons was completed for the beryllium cube with a characteristic dimension of 60 cm. The parasitic absorption was simulated by boron with level of 5 ppm. Calculation results for time dependence of the thermal neutron density are presented in Fig. 2. As shown, a fundamental difference is obtained in this case. The decay constant is a sensitive and a precise parameter from the media absorption property point of view. In favorable cases, experimental evaluation of time constant can achieve accuracy as high as 0.2%.

5.2. Experimental Arrangement

The experimental equipment consists of a pulsed D-T neutron source (FNS facility, JAERI), a beryllium assembly, a BF_3 neutron detector, and a time analyzer. An 80-degree beam line in the first target room of the FNS facility was used for the present experiment. The first target room provides the good experimental conditions from the neutron background point of view, due to the large size of the target room (15x15x12 m). The general setup of the experimental equipment and blocks of electronic equipment is shown in Fig. 3.

5.2.1. Pulsed Neutron Source and the Beryllium Assemblies

The target of the pulsed neutron source and the beryllium assembly is shown in Fig. 4. The neutron source pulse mode was configured by the following:

- ✓ D-T neutron burst width - 1 μsec;
- ✓ burst repetition time - 5 ms.

The distance between the neutron source and the surface of the assembly was about 50 mm. The pulsed source and the detector were located outside of the beryllium blocks, in the middle of the adjacent side planes. The shown arrangement minimizes the amount of higher harmonics contamination of the thermal neutrons decay [8].

Standard grade beryllium blocks (S-200F, Brush Wellman Inc.) were used to construct ninth prism assemblies. Main dimensions and buckling parameters for the assemblies are listed in Table 7.

Table 7

Beryllium assembly parameters used in the pulsed neutron experiment

Assembly Number	Assembly size, cm			Buckling parameter, cm^{-2}
	A Depth	B Width	C Height	
1	60.96	60.96	55.88	7.892E-3
2	53.34	60.96	55.88	8.620E-3
3	45.72	60.96	55.88	9.723E-3
4	38.10	60.96	55.88	1.151E-2
5	30.48	60.96	55.88	1.469E-2
6	50.80	50.80	50.8	1.057E-2
7	45.72	45.72	45.72	1.293E-2
8	40.64	40.64	40.64	1.619E-2
9	35.56	35.56	35.56	2.084E-2

The buckling parameter was estimated using the equation (4).

5.2.2. Effect of Backscattering Neutrons

Hence, backscattering neutrons can affect determination of the decay constant. An appropriate study was completed to verify this effect. Backscattering neutrons represent leakage neutrons from the experimental assembly, which are scattered by the concrete wall of the experimental room. Some of these neutrons return to the experimental assembly. The influence of neutrons, returned to the assembly, was examined by the Monte Carlo calculation. A concrete wall with a thickness of 0.5 m, was modeled to be 5.5 m apart from the D-T neutron source, which is the minimum distance from the D-T neutron source to the concrete wall. Figure 5 shows the reaction rate of the BF_3 detector ratio with and without the concrete wall. The influence of neutrons, returned to the assembly, was negligible small for the acquiring time interval of 1 – 2.5 ms.

5.3. Measurements

Thermal neutrons diffusing out of the beryllium assembly are detected with a BF_3 counter. Signals from the neutron detector are fed into a time analyzer. The decay curve was accumulated in the 256 channel time analyzer using a 20 μsec channel width. Several hundred thousands of counts were collected for each determination of the decay curve. Figures 6-8 show the decay curve for three assemblies: one of the largest, one of the medium and the smallest. Each decay curve was treated off-line.

5.3.1. Decay Rate of the Thermal Neutrons

A precise determination of the decay constant of various beryllium assemblies must be done with particular attention to the following main points:

- ✓ A small background of neutrons is always present, perhaps due to the fact that the neutron-producing deuterium beam cannot be completely cut off during the measurement period;
- ✓ Faster decays are superposed on the main decay.

In order to eliminate the background of neutrons, the treatment procedure for the decay curve was adapted. Prior to analysis, the difference between two successive channel counts was calculated, and the modified decay curve was used for determination of the decay constant. This procedure eliminates any bias, due to a constant background.

As stated earlier it is necessary to suppress the higher harmonics. It is evident (fig. 6-8), that the first channels of the decay curve are off the straight line, due to the contribution of the faster decays. The contribution of higher harmonics to the fundamental decay constant was mostly eliminated by proper arrangement of the neutron source and the detector (as mentioned before), and a proper choice of the delay time and duration period. The experimental decay curves were analyzed with different delays and durations in the time interval from 0.4 to 4. 5 msec after the neutron burst. The analyzed time conditions are listed in Table 8.

Table 8.

Time intervals for analysis of the decay curve.

Time interval number	Time interval, msec		Duration, msec
	From	To	
1	0.4	3.4	3.0
2	0.5	3.4	2.9
3	0.6	3.4	2.8
4	0.8	3.4	2.6
5	1.0	3.4	2.4
6	1.2	3.4	2.2
7	1.4	3.4	2.0
8	1.6	3.4	1.8
9	1.4	3.0	1.6
10	1.4	3.2	1.8
11	1.4	3.6	2.2
12	1.4	3.8	2.4
13	1.4	4.0	2.6
14	1.4	4.4	3.0
15	1.0	4.5	3.5

Figure 9 illustrates the dependence of the fundamental constant on the time interval number. Since the decay constants of the higher harmonics are larger than constant of the fundamental, higher modes will disappear faster than the fundamental mode. Thus, it is possible to obtain the value of the fundamental mode in the appropriate time intervals. By analyzing such kind of dependences for other beryllium assemblies, results of the decay constant were obtained, presented in Table 9.

Table 9.

Experimental decay constants

Assembly number	Dimensions, cm			Buckling parameter, cm^{-2}	Decay constant, sec^{-1}
	A Depth	B Width	C Height		
1	60.96	60.96	55.88	7.892×10^{-3}	1204±4
2	53.34	60.96	55.88	8.620×10^{-3}	1295±5
3	45.72	60.96	55.88	9.723×10^{-3}	1432±4
4	38.10	60.96	55.88	1.151×10^{-2}	1636±8
5	30.48	60.96	55.88	1.469×10^{-2}	1980±10
6	50.80	50.80	50.80	1.057×10^{-2}	1513±8
7	45.72	45.72	45.72	1.293×10^{-2}	1801±10
8	40.64	40.64	46.64	1.619×10^{-2}	2157±13
9	35.56	35.56	35.56	2.084×10^{-2}	2651±19

5.3.2. Macroscopic Absorption Cross Section

By analyzing the dependence of the experimental decay constants on assemblies of various sizes on the geometrical buckling, the total macroscopic absorption cross section was evaluated. Figure 10 shows a plot of the decay constant as a function of the geometrical buckling. According to the function (2), a parabola has been fitted to experimental points by the method of least squares. The diffusion parameters in beryllium, taken from the reference [8] and used as the coefficients of this parabola, were the following: $D = 1.21\times10^{5}$ cm^2/sec; $C = 3.68\times10^{5}$ cm^4/sec. Thus, the decay constant for an infinite medium was evaluated as $\alpha_0^{exp} = 278\pm25$ sec^{-1}. Assuming that the absorption follows the 1/v law, calculation of the macroscopic absorption cross section with formula (3) gives the value of $(1.26\pm0.11)\times10^{-3}$ cm^{-1}.

5.4. MCNP Calculations

Experimental results were calculated by the Monte Carlo Neutral Particle transport code MCNP-4B with the Japanese Evaluated Nuclear Data Library JENDL-3.2 and JENDL Dosimetry File. Manufacturer information on major impurities (C, O, Al and Fe) was taken into account. Figures 11 and 12 show results of calculations for beryllium assemblies with dimensions of approximately 30×30×30 up to 60×60×60 cm.

5.5. Comparisons of the Calculated and Experimental data

Two independent comparisons were completed, based on the experimental and calculated results. First of all, the measured decay curves of the thermal neutrons diffusing out of the beryllium assembly, were compared with the Monte Carlo calculations. A comparison example for the beryllium assembly with a size of about 60×60×60 cm is shown in Fig. 13. It is evident that the measured decay curve was faster than the calculated curve. Similar results were obtained for all ninth assemblies, indicating, that thermal neutrons are absorbed by minor impurities present in beryllium blocks.

In addition, the experimental macroscopic cross section and the appropriate calculated value were compared. The calculated value, $\Sigma_a^{cal} = 9.95\times10^{-4}$ cm^{-1}, was based on the absorption cross section data for beryllium and impurity elements taken from the JENDL -3.3 library [9], and chemical composition of beryllium, provided by the manufacturing company, Table 4. The experimental value of the macroscopic absorption cross section was evaluated as $\Sigma_a^{exp} = (1.26\pm0.11)\times10^{-3}$ cm^{-1}. Comparison of these values indicates, that the experimental value is about 30% higher than the value based on the reference data. This result is consistent with the observation for experimental and calculated decay curves.

6. Conclusion

Structural beryllium (S-65C, S-200F, S-200E form Brush Wellman Inc.), which is considered for use in ITER, contains unspecified impurities with a total amount of less than 400 ppm. The composition of these impurities contains elements, such as Li, B, Cd and others, which can affect the tritium breeding ratio, due to the parasitic absorption of thermal neutrons in the beryllium material, even if their content is less than 10 ppm. The sample and integral analysis were completed in order to gain information on unspecified impurities. Sample analysis was completed by the ICP-MS method, and the integral analysis – by the neutron pulsed method. The latter non-destructive method is very effective and sensitive to impurities, which affect the evaluation of the tritium breeding ratio. Results obtained in these analyses are in a reasonably good agreement. Presented measurements demonstrated the effectiveness of the pulsed neutron method, as a tool, ideal for fast and simple determination of the integral effect of impurities. It has been experimentally proven, that the effective absorption of thermal neutrons in structural beryllium (S-200F) is approximately 30% higher than the calculated value, based on the data, specified by the manufacturing company. For the pure beryllium assembly, such effect will decrease the tritium production rate by at least 5 %. In the blanket of a fusion reactor, the effect will depend on the blanket design, volumetric ratio of lithium and beryllium, and enrichment of the lithium. The estimation should be completed in each case.

7. Additional Remarks

Acquiring the impurity information is not only important for evaluation of the tritium breeding ratio, it is also significant for studies concerning the activation and transmutation behavior of beryllium in future fusion power plants. The activation behavior of beryllium in a fusion reactor depends strongly on the presence of impurities in the metal, thus affecting the choice of conditioning methods for beryllium waste from fusion reactors. Estimations [10] show, that the radiotoxicity, and the actinide inventory of the fusion beryllium waste, are strongly associated with initial concentrations of uranium and thorium.

Acknowledgments

The authors gratefully acknowledge M. Ito for analysis of the beryllium sample, C. Kutsukake, S. Tanaka, Y. Abe, M. Seki and Y. Oginuma, for their excellent operation of the D-T pulsed neutron source at the FNS facility.

References

[1] M. Enoeda, Y. Kosaku, T. Hatano, T. Kuroda, N. Miki, T. Honma, and M. Akiba, Design and technology development of solid breeder blanket cooled by supercritical water in Japan, FT/P1-08, Fusion Energy 2002 (Proc. 19th Fusion Energy Conference, Lyon, 2002) (Vienna IAEA), CD-ROM file FT/P1-08, http://www.iaea.org/programmes/ripc/physics/fec2002/html/fec2002.htm

[2] C.R. Tipton (Ed.), Reactor handbook, second ed., Interscience Publishers, Inc., New York, pp. 897-898 (1960).

[3] D. E. Dombrowski, Manufacture of beryllium for fusion applications. Fusion Eng. Des. 37, 229-242 (1997).

[4] A.A. Smales, D. Mapper, A.P. Seyfang, The determination of uranium in fairly pure beryllium metal by neutron activation and gamma spectrometry. Analytica Chimica Acta. 25, 587-597 (1961).

[5] G.E. Darwin, J.H. Buddery, Beryllium, Butterworths Scientific Publications, London (1960).

[6] D. Webster, G.J. London (Eds.), Beryllium Science and Technology, V. 1, Plenum Press, New York, pp. 34-36 (1979).

[7] M. Ito, JAERI, private communication (2003).

[8] K.H. Beckurts, K. Wirtz, Neutron Physics, Spriger-Verlag, Berlin (1964).

[9] T. Nakagawa, H. Kawasaki, K. Shibata (Eds.), Curves and Tables of Neutron Cross Sections in JENDL –3.3, Japan Atomic Energy Research Institute Report, JAERI-Data/Code 2002-020 (2002).

[10] F. Druyts, P. Van Iseghem, Conditioning methods for beryllium waste from fusion reactors, Fusion Eng. Des. 69 607-610 (2003).

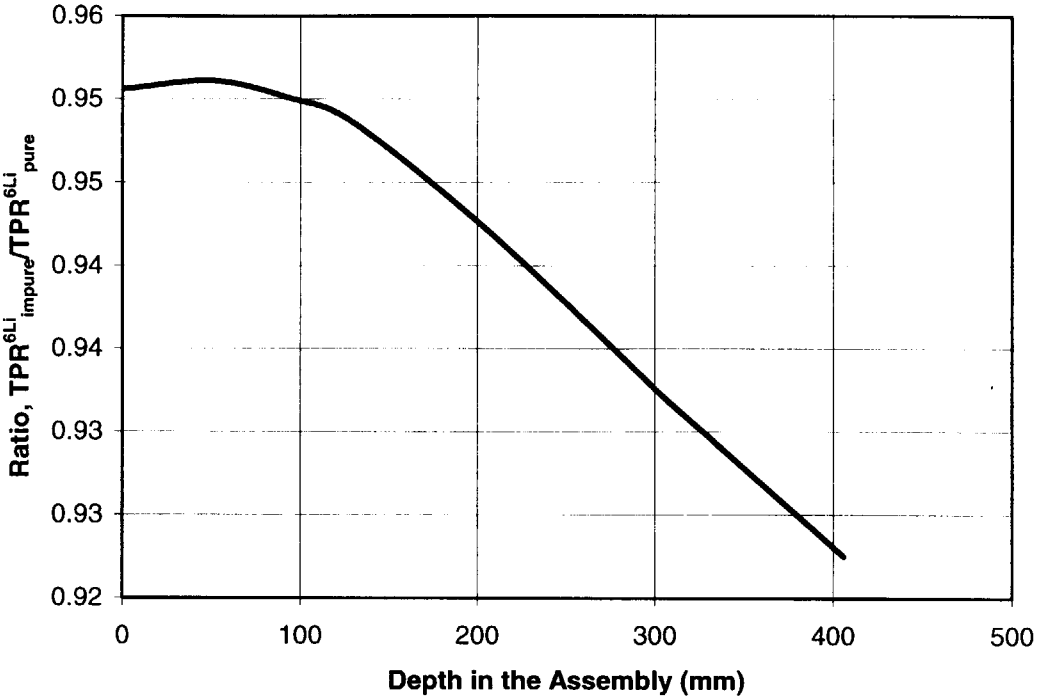

Figure 1. The parasitic absorption effect in the beryllium bulk assembly on the tritium production rate, produced on lithium-6.

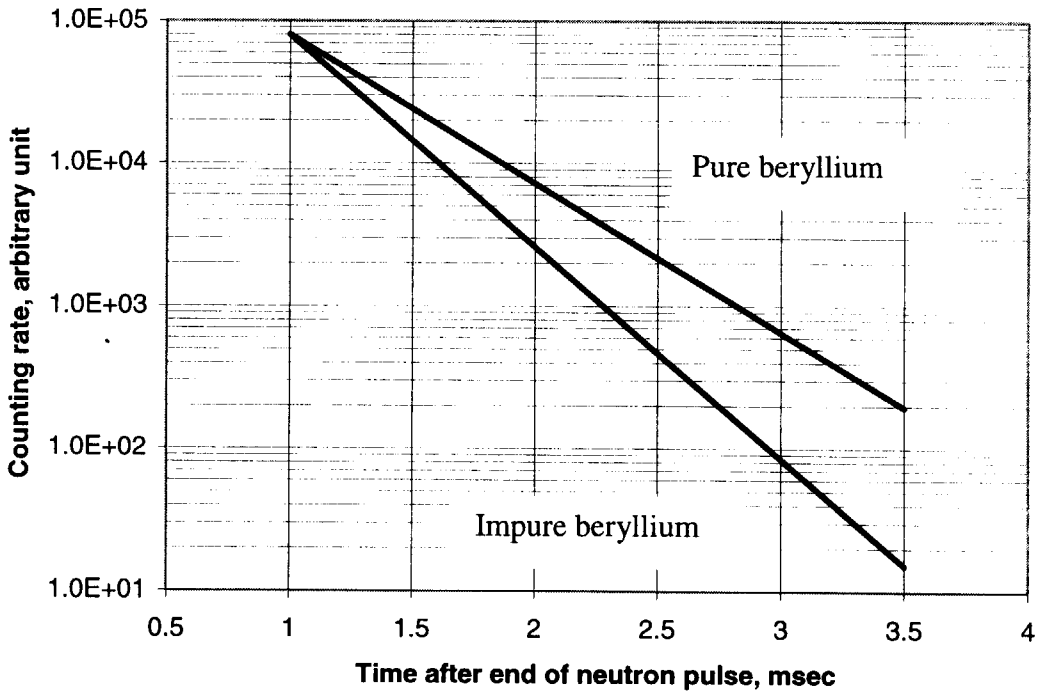

Figure 2. The parasitic absorption effect in the beryllium on the time behaviour of the thermal neutrons, diffusing out of beryllium assembly.

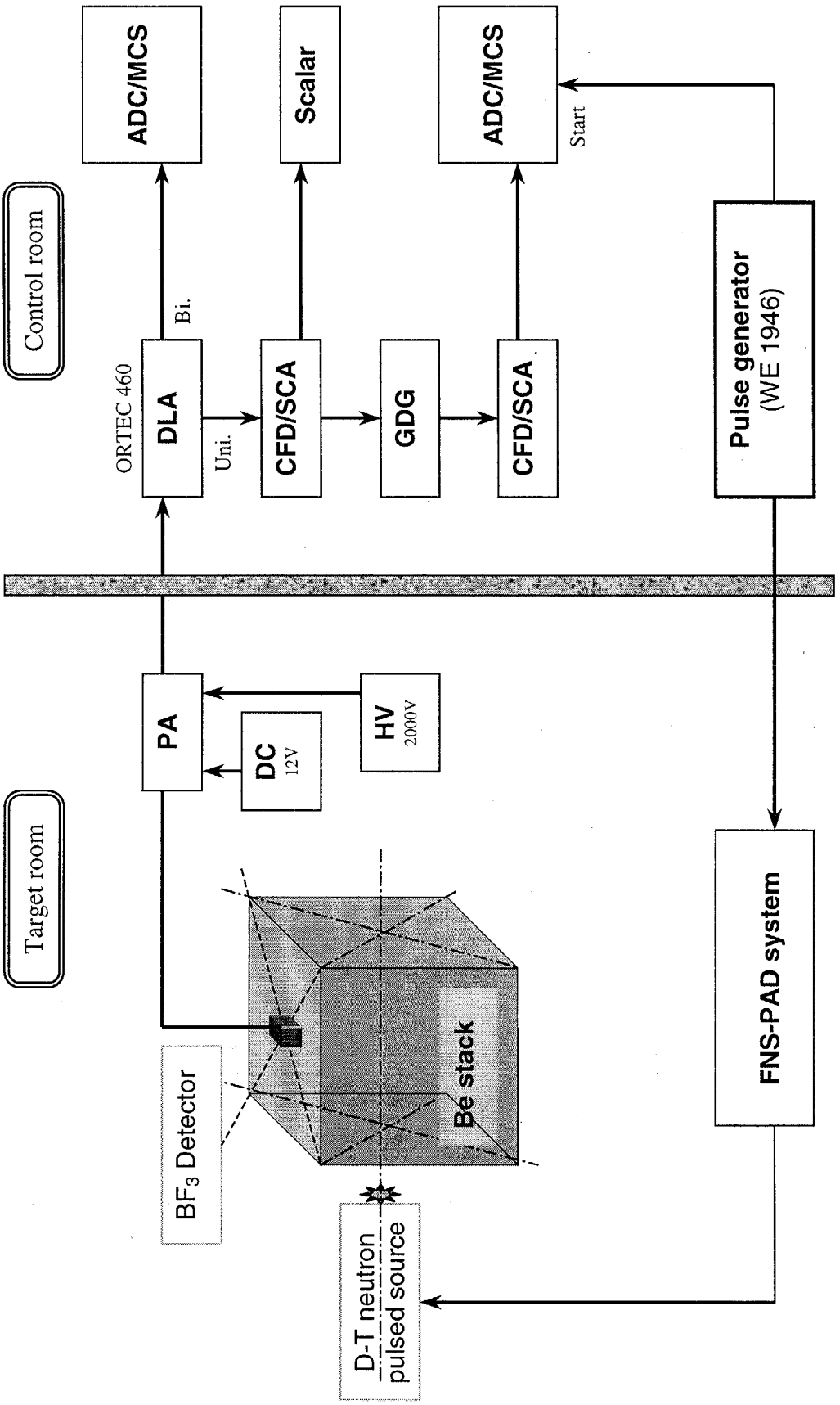

Figure 3. Schematic diagram of the neutron pulsed experiment with the beryllium assembly.

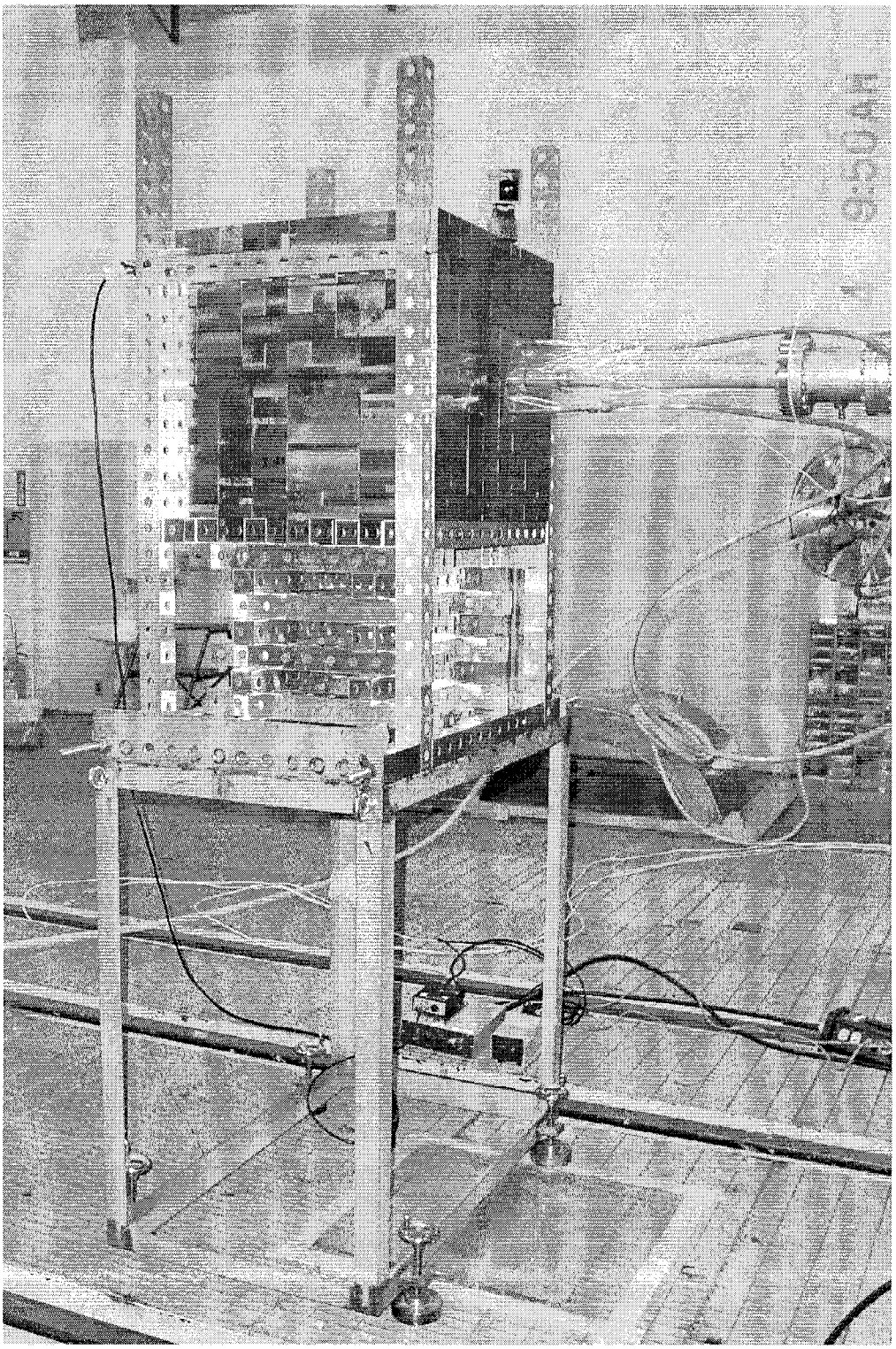

Figure 4. Beryllium assembly and the neutron target in the first experimental room.

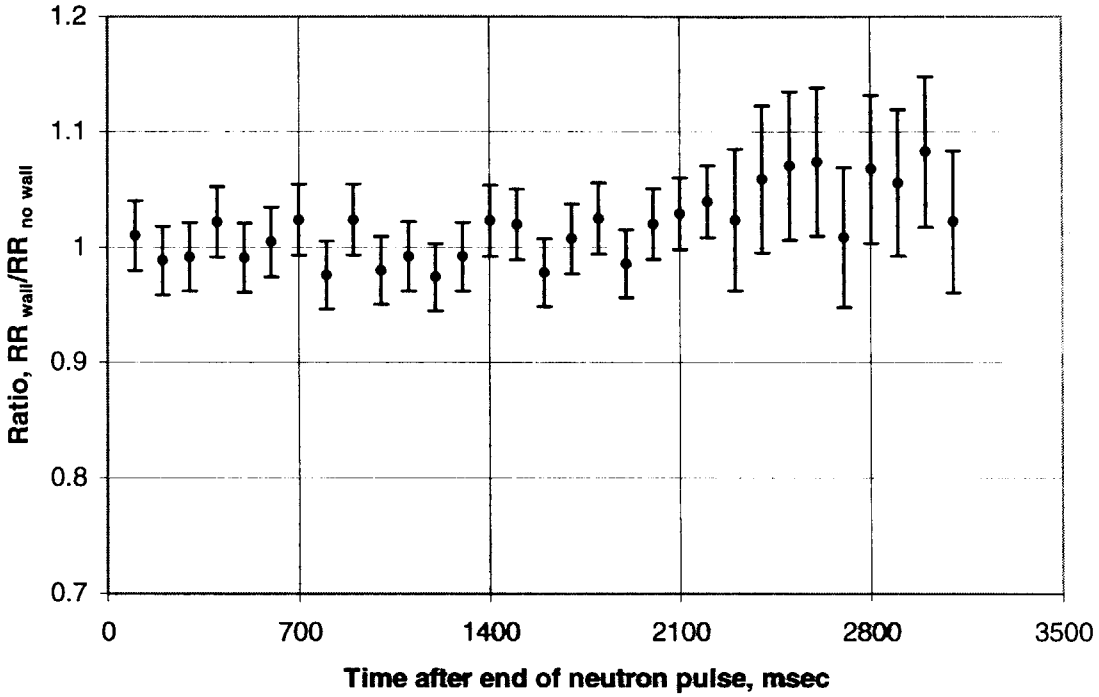

Figure 5. Calculated ratio of the $^{10}B(n,t)^{7}Li$ reaction rate for different conditions: with and without the concrete wall of the experimental room.

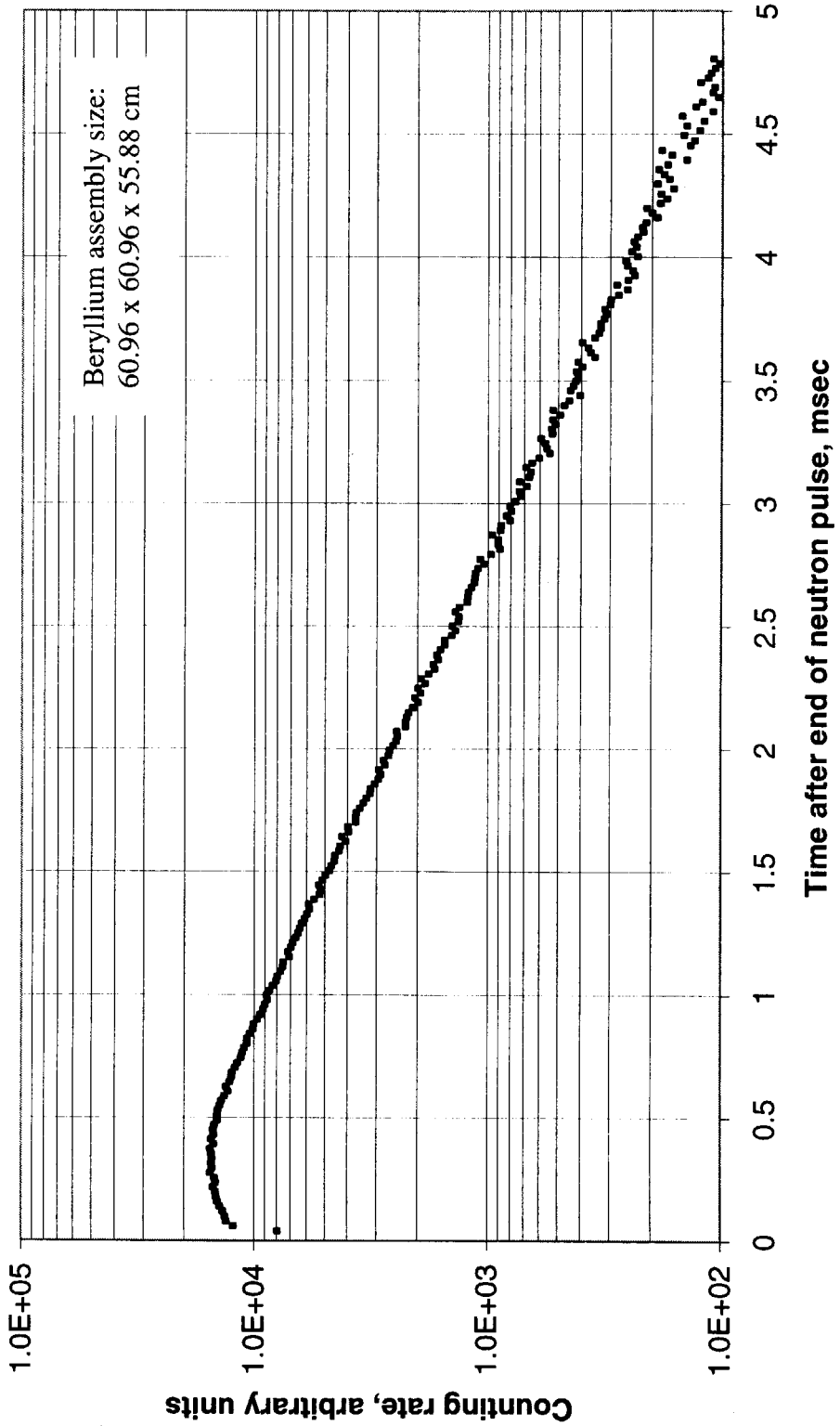

Figure 6. The decay curve of thermal neutrons diffusing out of the beryllium assembly, as detected with a BF_3 counter.

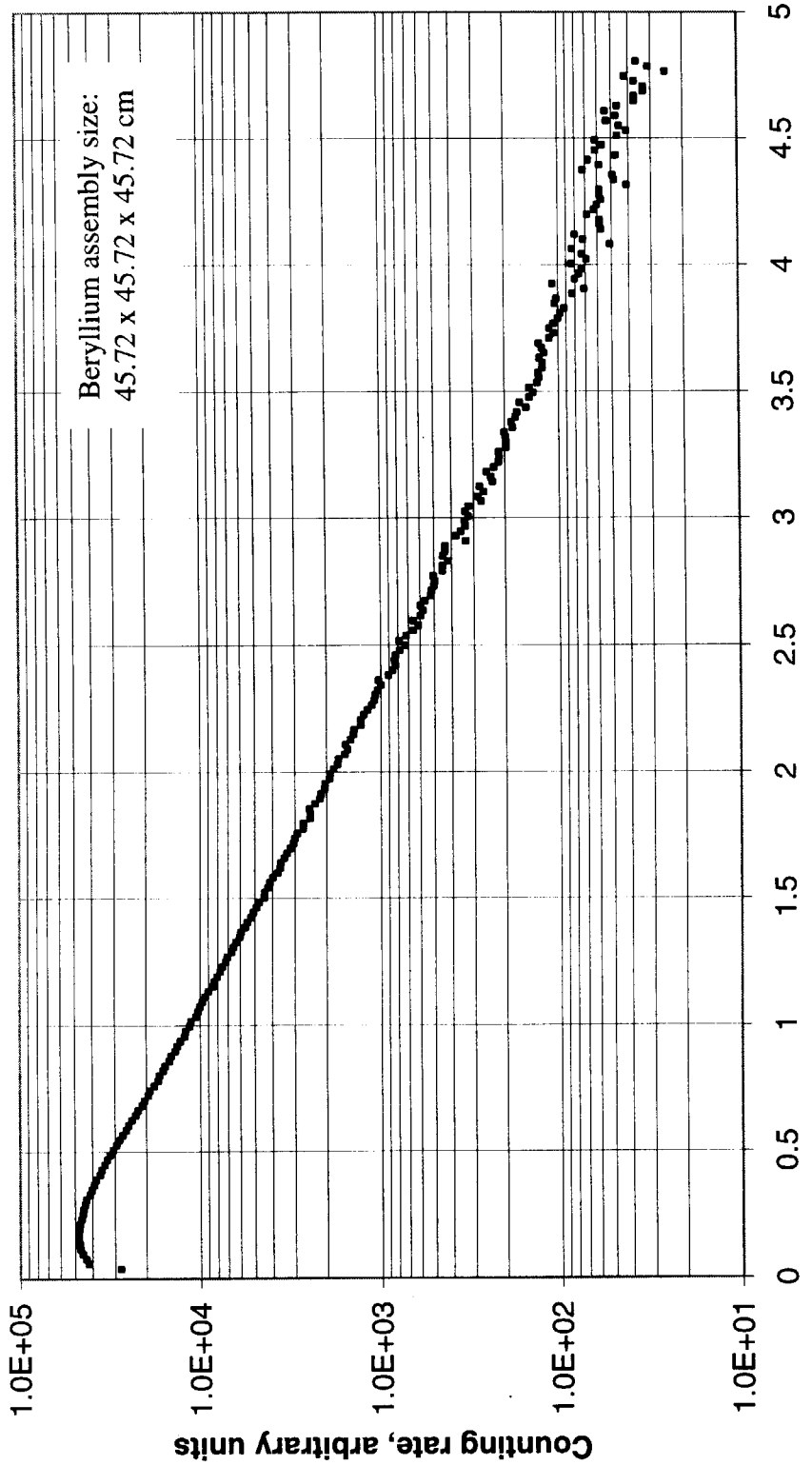

Figure 7. The decay curve of thermal neutrons diffusing out of the beryllium assembly, as detected with a BF_3 counter.

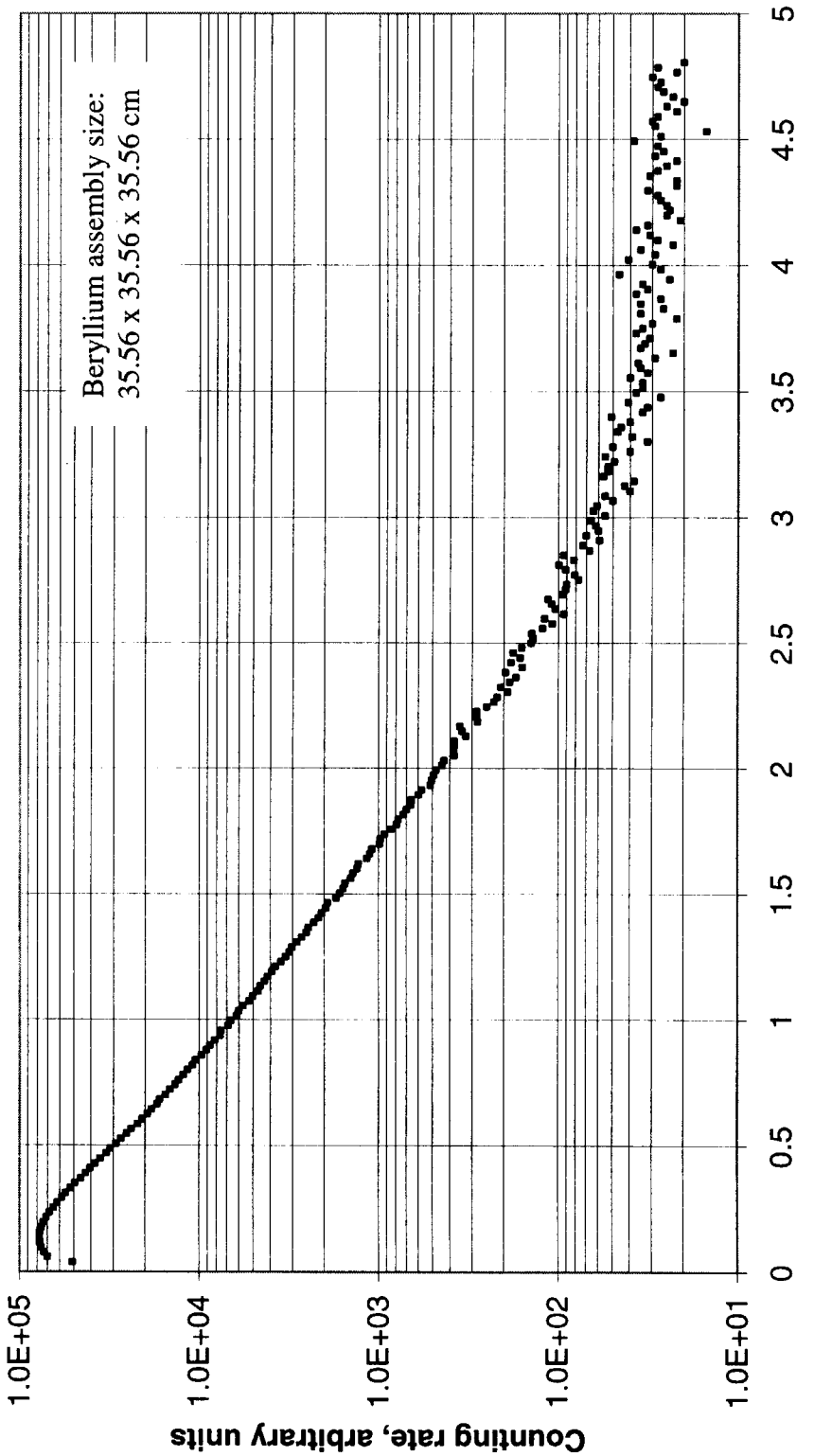

Figure 8. The decay curve of thermal neutrons diffusing out of the beryllium assembly, as detected with a BF_3 counter.

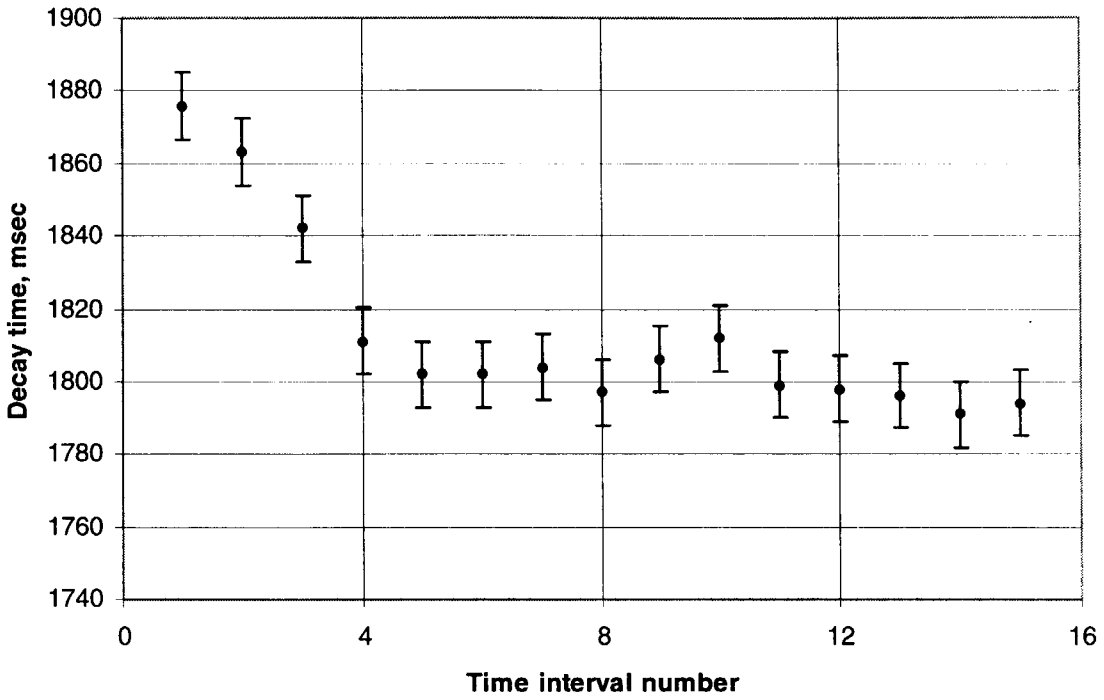

Figure 9. Dependence of the fundamental decay constant on the time interval number for beryllium assembly dimensions of 45.72 x 45.72 x 45.72 cm.

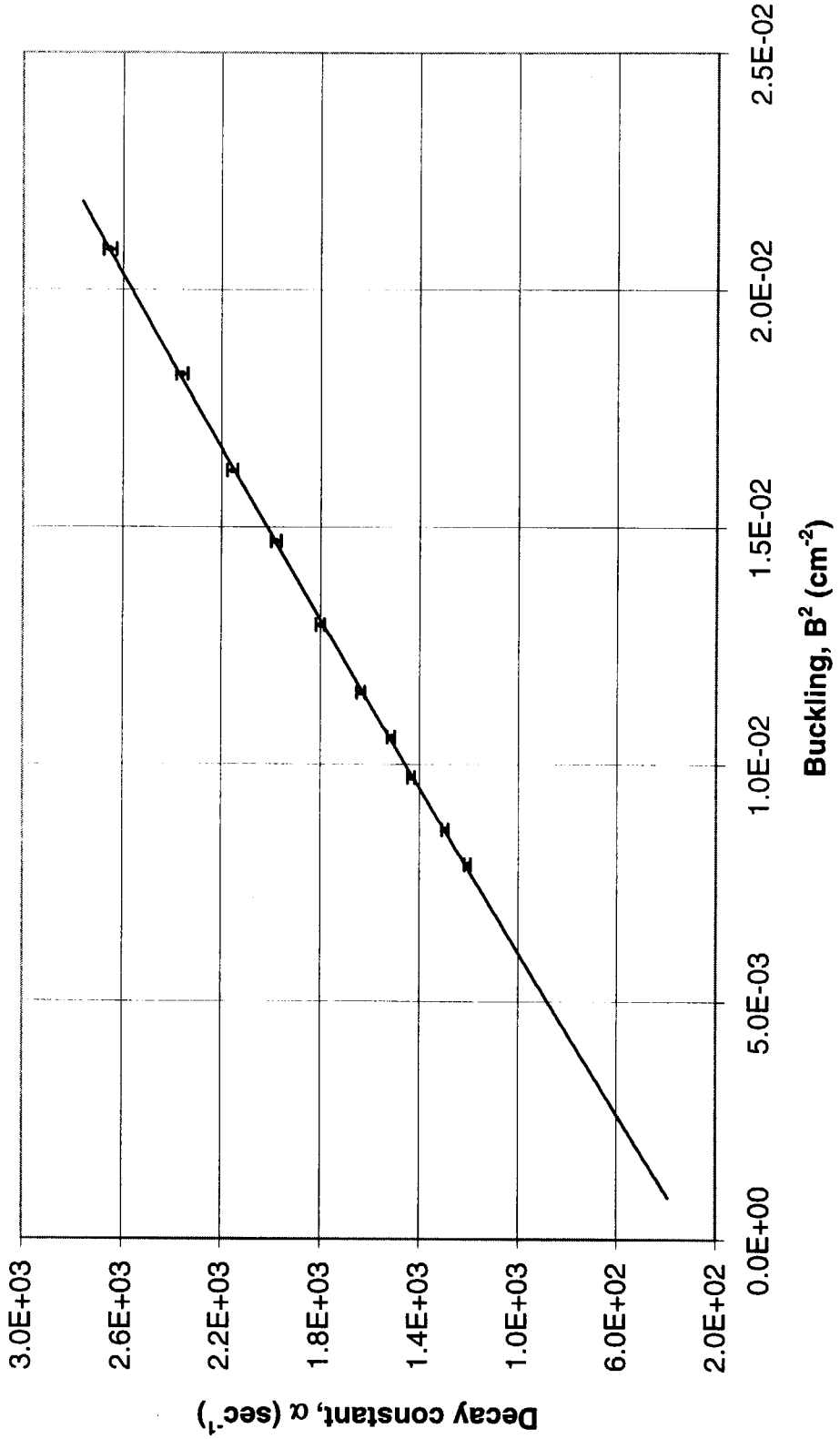

Figure 10. Thermal neutron decay constant as a function of geometrical buckling for room temperature beryllium.

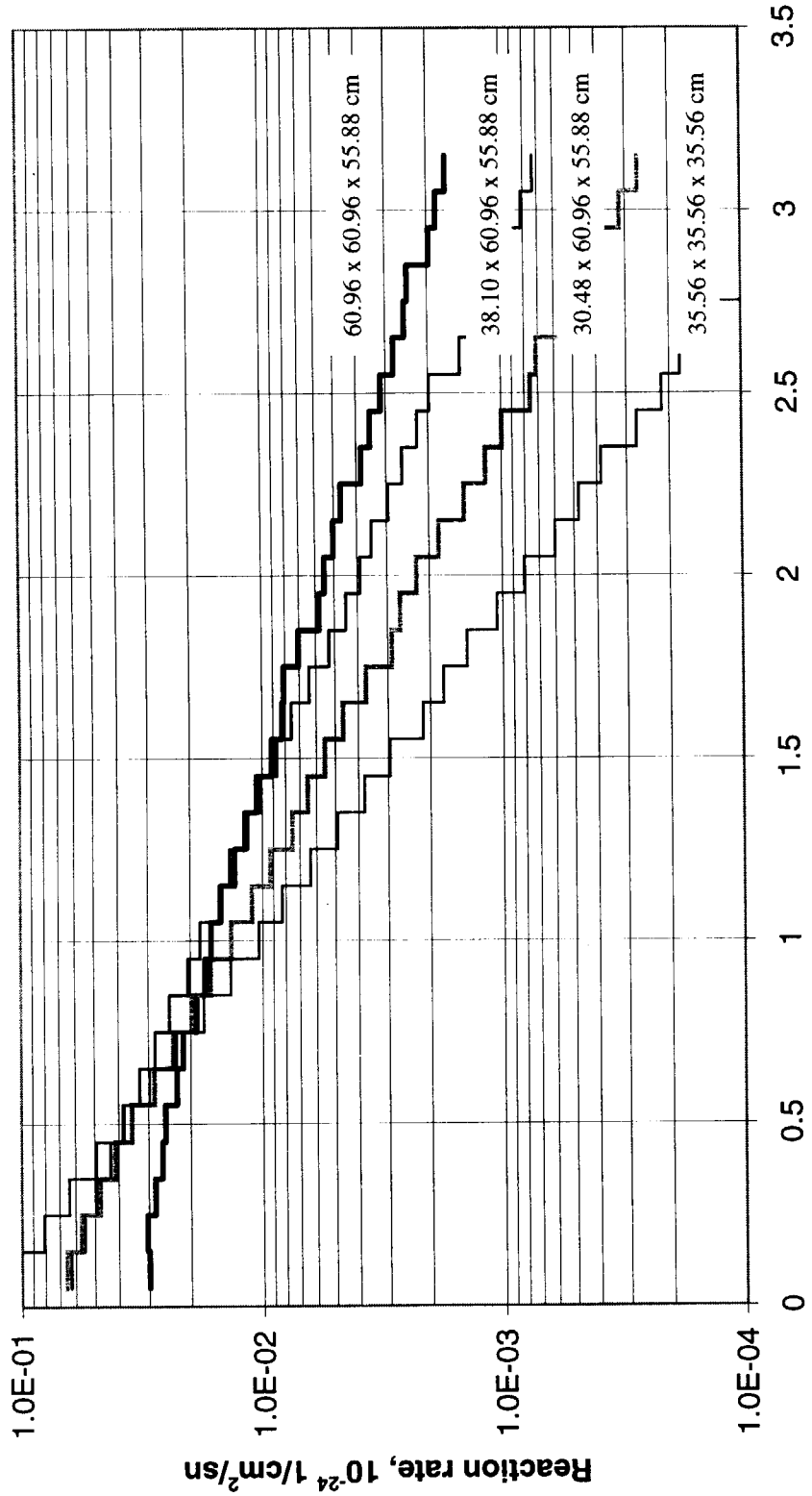

Figure 11. The calculated time-dependent reaction rate of $^{10}B(n,t)^{7}Li$ for thermal neutrons diffusing out of beryllium assembly with different dimensions.

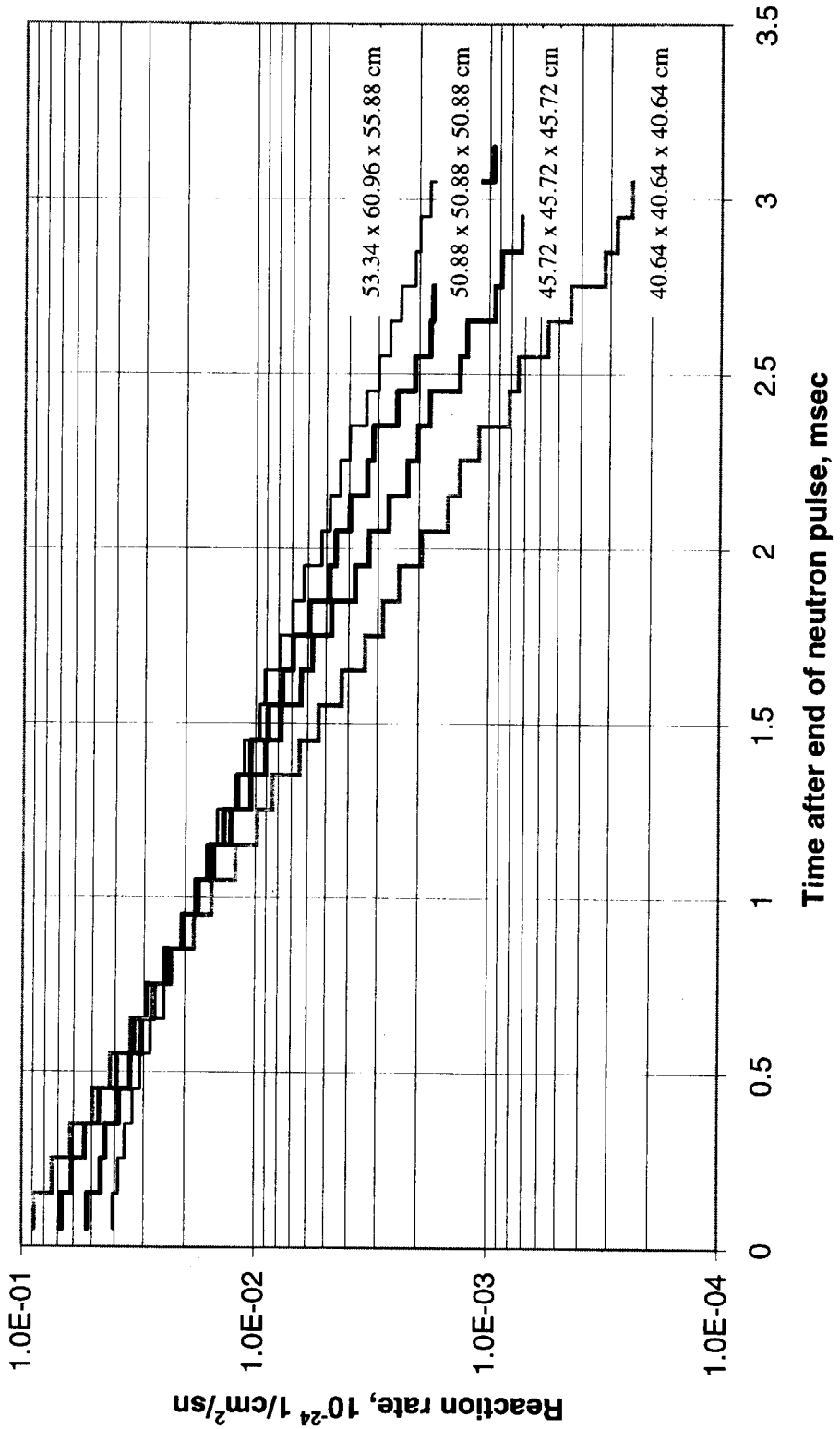

Figure 12. The calculated time-dependent reaction rate of $^{10}B(n,t)^7Li$ for thermal neutrons diffusing out of beryllium assembly with different dimensions.

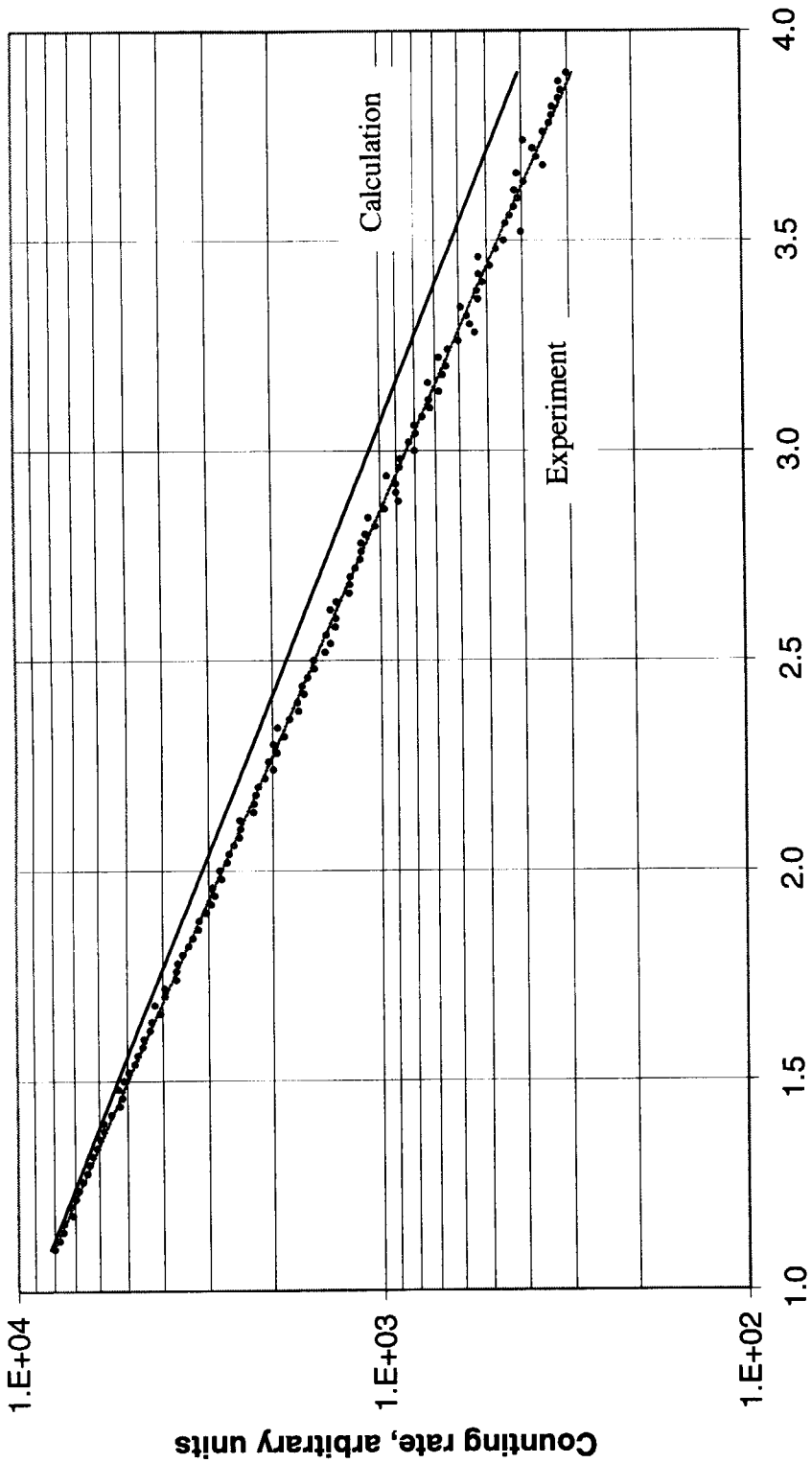

Figure 13. Comparison of the experimental and the calculated decay curve of thermal neutrons diffusion out of the beryllium assembly, as detected with the BF_3 counter.

国際単位系（SI）と換算表

表1　SI基本単位および補助単位

量	名称	記号
長さ	メートル	m
質量	キログラム	kg
時間	秒	s
電流	アンペア	A
熱力学温度	ケルビン	K
物質量	モル	mol
光度	カンデラ	cd
平面角	ラジアン	rad
立体角	ステラジアン	sr

表2　SIと併用される単位

名称	記号
分，時，日	min，h，d
度，分，秒	°，′，″
リットル	l，L
トン	t
電子ボルト	eV
原子質量単位	u

1 eV=1.60218×10^{-19}J

1 u=1.66054×10^{-27}kg

表3　固有の名称をもつSI組立単位

量	名称	記号	他のSI単位による表現
周波数	ヘルツ	Hz	s^{-1}
力	ニュートン	N	$m\cdot kg/s^2$
圧力，応力	パスカル	Pa	N/m^2
エネルギー，仕事，熱量	ジュール	J	N·m
工率，放射束	ワット	W	J/s
電気量，電荷	クーロン	C	A·s
電位，電圧，起電力	ボルト	V	W/A
静電容量	ファラド	F	C/V
電気抵抗	オーム	Ω	V/A
コンダクタンス	ジーメンス	S	A/V
磁束	ウェーバ	Wb	V·s
磁束密度	テスラ	T	Wb/m^2
インダクタンス	ヘンリー	H	Wb/A
セルシウス温度	セルシウス度	℃	
光束	ルーメン	lm	cd·sr
照度	ルクス	lx	lm/m^2
放射能	ベクレル	Bq	s^{-1}
吸収線量	グレイ	Gy	J/kg
線量等量	シーベルト	Sv	J/kg

表4　SIと共に暫定的に維持される単位

名称	記号
オングストローム	Å
バーン	b
バール	bar
ガル	Gal
キュリー	Ci
レントゲン	R
ラド	rad
レム	rem

1 Å=0.1nm=10^{-10}m

1 b=100fm^2=10^{-28}m^2

1 bar=0.1MPa=10^{5}Pa

1 Gal=1cm/s^2=10^{-2}m/s^2

1 Ci=3.7×10^{10}Bq

1 R=2.58×10^{-4}C/kg

1 rad=1cGy=10^{-2}Gy

1 rem=1cSv=10^{-2}Sv

表5　SI接頭語

倍数	接頭語	記号
10^{18}	エクサ	E
10^{15}	ペタ	P
10^{12}	テラ	T
10^{9}	ギガ	G
10^{6}	メガ	M
10^{3}	キロ	k
10^{2}	ヘクト	h
10^{1}	デカ	da
10^{-1}	デシ	d
10^{-2}	センチ	c
10^{-3}	ミリ	m
10^{-6}	マイクロ	μ
10^{-9}	ナノ	n
10^{-12}	ピコ	p
10^{-15}	フェムト	f
10^{-18}	アト	a

（注）

1．表1－5は「国際単位系」第5版，国際度量衡局1985年刊行による。ただし，1 eVおよび1 uの値はCODATAの1986年推奨値によった。

2．表4には海里，ノット，アール，ヘクタールも含まれているが日常の単位なのでここでは省略した。

3．barは，JISでは流体の圧力を表わす場合に限り表2のカテゴリーに分類されている。

4．EC閣僚理事会指令ではbar，barnおよび「血圧の単位」mmHgを表2のカテゴリーに入れている。

換算表

	N(=10^{5}dyn)	kgf	lbf
力	1	0.101972	0.224809
	9.80665	1	2.20462
	4.44822	0.453592	1

粘度　1 Pa·s(N·s/m^2)=10 P(ポアズ)(g/(cm·s))

動粘度　1m^2/s=10^{4}St(ストークス)(cm^2/s)

	MPa(=10bar)	kgf/cm^2	atm	mmHg(Torr)	lbf/in^2(psi)
圧力	1	10.1972	9.86923	7.50062×10^3	145.038
	0.0980665	1	0.967841	735.559	14.2233
	0.101325	1.03323	1	760	14.6959
	1.33322×10^{-4}	1.35951×10^{-3}	1.31579×10^{-3}	1	1.93368×10^{-2}
	6.89476×10^{-3}	7.03070×10^{-2}	6.80460×10^{-2}	51.7149	1

	J(=10^7 erg)	kgf·m	kW·h	cal(計量法)	Btu	ft·lbf	eV
エネルギー・仕事・熱量	1	0.101972	2.77778×10^{-7}	0.238889	9.47813×10^{-4}	0.737562	6.24150×10^{18}
	9.80665	1	2.72407×10^{-6}	2.34270	9.29487×10^{-3}	7.23301	6.12082×10^{19}
	3.6×10^6	3.67098×10^5	1	8.59999×10^5	3412.13	2.65522×10^6	2.24694×10^{25}
	4.18605	0.426858	1.16279×10^{-6}	1	3.96759×10^{-3}	3.08747	2.61272×10^{19}
	1055.06	107.586	2.93072×10^{-4}	252.042	1	778.172	6.58515×10^{21}
	1.35582	0.138255	3.76616×10^{-7}	0.323890	1.28506×10^{-3}	1	8.46233×10^{18}
	1.60218×10^{-19}	1.63377×10^{-20}	4.45050×10^{-26}	3.82743×10^{-20}	1.51857×10^{-22}	1.18171×10^{-19}	1

1 cal= 4.18605J（計量法）

= 4.184J（熱化学）

= 4.1855J（15℃）

= 4.1868J（国際蒸気表）

仕事率　1 PS(仏馬力)

= 75 kgf·m/s

= 735.499W

放射能	Bq	Ci
	1	2.70270×10^{-11}
	3.7×10^{10}	1

吸収線量	Gy	rad
	1	100
	0.01	1

照射線量	C/kg	R
	1	3876
	2.58×10^{-4}	1

線量当量	Sv	rem
	1	100
	0.01	1

（86年12月26日現在）

Analysis of Impurities in Beryllium, Affecting Evaluation of the Tritium Breeding Ratio